Ferrocene and Dicarbonylcyclopentadienylcobalt in Faujasite-Type Zeolites: A Study of Molecular Motion

A. R. Overweg,*,† H. Koller,‡ J. W. de Haan,† L. J. M. van de Ven,† A. M. van der Kraan,§ and R. A. van Santen†

Schuit Insitute of Catalysis, Laboratory of Inorganic Chemistry and Catalysis, Eindhoven University of Technology, P.O. Box 513, 5600 MB Eindhoven, The Netherlands, Institute of Physical Chemistry, University of Münster, Schlossplatz 4/7, 48149 Münster, Germany, and Interfacultair Reactor Instituut, Delft University of Technology, Mekelweg 15, 2629 JB Delft, The Netherlands

Received: November 23, 1998; In Final Form: March 9, 1999

The anisotropic molecular motion of $Fe(C_5H_5)_2$ and $Co(C_5H_5)(CO)_2$ molecules in the supercages of faujasite-type zeolites has been examined by NMR and by Mössbauer spectroscopy. Static ^2H quad-echo and $\{^1H\text{-}\}^{13}C$ CP NMR techniques show that below 225 K the $Fe(C_5H_5)_2$ molecules have no translational freedom, the only motion being rapid rotation of the cyclopentadienyl rings about their 5-fold axes. This is indicated by an axially symmetric powder pattern ($\delta_{iso} = 69.7$ ppm, $\Omega = 75.0$ ppm) in the $\{^1H\text{-}\}^{13}C$ CP NMR spectrum and a broad Pake-type powder pattern (QCC = 97.3 kHz) in the ^2H NMR spectrum. As the temperature is raised the molecules gain translational freedom, and at temperatures above 358 K isotropic molecular motion is identified as the only type of molecular motion. A model is proposed suggesting that the translational, isotropic motion is mainly caused by *intra*cage, SII→SII jumps of the $Fe(C_5H_5)_2$ molecules. Based on this model activation energies and diffusion coefficients were calculated from the NMR parameters. The molecular motion of intrazeolite $Fe(C_5H_5)_2$ depends on the Si/Al ratio of the Na-faujasite host as well, being the highest for Na-faujasites with the lowest Si/Al ratio. The higher amount of sodium cations in the supercages probably causes a decrease in the energy barriers for site-to-site hopping. $\{^1H\text{-}\}^{13}C$ CP NMR experiments show that $Co(C_5H_5)(CO)_2$ molecules get firmly fixed in the zeolite at 183 K. This observation enabled the study of the OC−Co−CO bite angle, φ, by use of ^{13}C Hahn-echo NMR experiments on enriched $Co(C_5H_5)(^{13}CO)_2$. The presence of an inverted axially symmetric powder pattern with span, Ω, of 127 ppm and a second powder pattern with $\Omega = 287$ ppm indicate changes in the bite angle.

Introduction

Confinement of transition metal complexes in the voids of zeolite host frameworks has gained considerable attention over the last years.[1−3] The motivation for the increasing interest for this type of materials stems from future prospects of applications in heterogeneous catalysis for electronic devices and optical materials. Several synthesis methods have been applied for the inclusion of molecular species in the crystallographically defined cavities of zeolites. Most of them rely on postsynthesis inclusion by diffusional processes. The empty cages of zeolites, which are prepared and calcined or dehydrated in a previous step, are loaded with the transition metal complex by ion exchange, vapor phase insertion, or ship-in-the-bottle synthesis. A very recent development is the incorporation of transition metal complexes by addition of the complex to the synthesis gel of the molecular sieve. The transition metal complex acts as a structure-directing agent during synthesis. In this way it has been shown that metallocene complexes successfully lead to a number of molecular sieves.[4−9]

Here, it is chosen to modify zeolites in a postsynthesis process by loading the molecular sieve with organometallic complexes via vapor phase insertion. Therefore, synthetic faujasite-type Y is chosen as the archetype zeolite because it contains large voids which can easily accommodate molecular species of reasonable size. The framework structure of the synthetic faujasite is illustrated in Figure 1. The black dots indicated in the Figure represent the possible cation positions. It is known from several studies that the extraframework cations play an important role in the interaction of the zeolite with the adsorbed molecular species.[10−12] For that reason, knowledge about the location and population of the cation positions is of great importance to the study of entrapped species in the cages of zeolites. The population of the sites is a function of the Si/Al ratio, the cation type, and the hydration state of the zeolite. It is found by both crystallographic[13−15] and spectroscopic[16] techniques that for dehydrated NaY zeolites (Si/Al > 2.4) the Na^+ ions are located on sites I, I′, and II. With decreasing Si/Al ratios (Si/Al < 2.0), further Na^+ ions are found on site III. Because of their size, organometallics can only enter the supercages of the faujasite structure. This implies that they interact predominantly with Na^+ ions on positions II and III.

The organometallics of choice in this work are $Fe(C_5H_5)_2$ and $Co(C_5H_5)(CO)_2$. $Fe(C_5H_5)_2$ is used to introduce iron in the voids of zeolites. The deposition of small iron particles in zeolitic materials is of great interest because of their potential use in catalytic processes that involve C−C bond formation, such as the Fischer−Tropsch process.[17] The classical preparation method, consisting of ion exchange followed by reduction, is

† Eindhoven University of Technology.
‡ University of Münster.
§ Delft University of Technology.

10.1021/jp984517x CCC: $18.00
Published on Web 05/08/1999

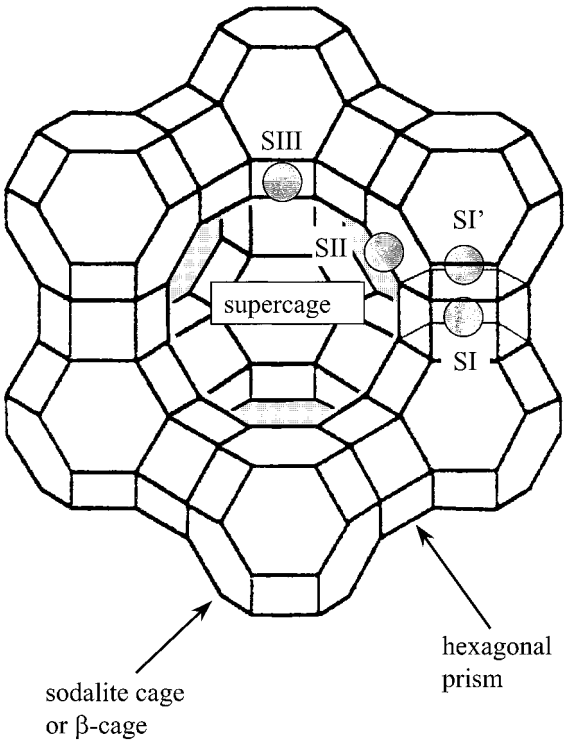

Figure 1. Framework structure of synthetic faujasite. The cation positions are indicated by the black dots.

hampered by the difficulty to reduce the cationic species to metallic iron.[18] Alternatively, neutral iron complexes, such as $Fe(CO)_5$[17,19,20] or $Fe(C_5H_5)_2$[21] can be placed in the cages of the zeolite by vapor phase insertion and subsequently decomposed. Apart from the fact that these organometallic compounds carry iron atoms in a low valence state, thus making a reduction step under severe conditions superfluous, they have the additional advantage that iron is deposited in the supercages, where it is accessible to substrate molecules.

The introduction of cobalt in the cages of zeolites is also a matter of great interest. In contrast to iron, more emphasis is put on the in situ, or ship-in-the-bottle synthesis of cobalt-containing complexes in the microporous materials. Much attention has been paid to the incorporation of Schiff base (e.g., salene) complexes,[22,23] porphyrin complexes,[24] and phthalocyanine complexes.[25,26] Studies focused on this subject have been motivated by the potential of controlled redox activity at the cobalt center of the intrazeolite complexes. The deposition of cobalt clusters in zeolite cages has been attempted by gas-phase insertion of $Co_2(CO)_8$.[27−29] This procedure, however, predominantly yielded cobalt carbonyl clusters deposited on the outer surface of the zeolite.

In this study, results are presented describing the interaction of zeolite NaY with $Co(C_5H_5)(CO)_2$. The incorporation of this complex into a number of zeolites Y with different extraframework cations has been studied earlier by Li et al.[30] and showed an interesting chemistry upon loading. In the case of NaY, two adsorption modes of the molecule were distinguished. One adsorption site involves the interaction of both carbonyl ligands each with a sodium cation. It was derived from the intensity of vibrational bands in the IR spectrum that this adsorption mode dominates over the other, which was assigned to an interaction between the cyclopentadienyl ring of the cobalt complex with a sodium cation in the supercage of the zeolite. Moreover, from the intensity of the υ_{CO} stretching modes, an estimate was made of the OC−Co−CO bite angle for the molecules which interact with the zeolite via the carbonyl ligands. A value of 106° was found for the intrazeolite complex compared to 98.4° for molecules in the gas phase.[31]

$Fe(C_5H_5)_2$ molecules, encaged in the voids of zeolites, have been characterized by several methods, IR and Raman spectroscopy and EXAFS, EPR, and Mössbauer spectroscopy. Ozin et al.[32] have studied the interaction of $Fe(C_5H_5)_2$, $Co(C_5H_5)_2$, and $Cr(C_5H_5)_2$ with both nonacidic NaY and partly exchanged acidic $H_nNa_{56-n}Y$ zeolites. They observed, using optical reflectance spectroscopy, a partial oxidation of $Fe(C_5H_5)_2$ upon insertion in the voids of NaY. It was concluded that defects in the zeolite lattice were responsible for this oxidation. A similar observation was made by Suib et al.,[33] who loaded ZSM-5 with $Fe(C_5H_5)_2$ molecules, and observed a partial oxidation as revealed by Mössbauer spectroscopy. They proposed that water was the oxidizing agent. Other studies originate from Dutta et al.[34] and Li et al.[35] The former studied the oxidation of $Fe(C_5H_5)_2$ to ferrocenium ions in zeolite Y by exposure to dry oxygen. Using Raman spectroscopy, they showed that the tendency of the intrazeolite $Fe(C_5H_5)_2$ molecules to oxidize is strongly influenced by the extraframework cation inside the zeolite cavities. Li et al. studied the capability of $Fe(C_5H_5)_2$, trapped in the supercages of a Y zeolite, to transfer electrons as a part of their goal to design chemically modified tinoxide electrodes.

To get a deeper understanding of the interaction of encaged $Fe(C_5H_5)_2$ and $Co(C_5H_5)(CO)_2$ with the faujasite zeolite, an investigation has been undertaken of the molecular motion of the complexes in the supercages of the zeolite. For this purpose use has been made of variable temperature ^2H and ^{13}C NMR experiments on stationary samples and of Mössbauer spectroscopy. The dynamics of $Fe(C_5H_5)_2$ in $Na_{55}Y$ is studied in detail, and we extended this study to synthetic faujasite NaY(X) zeolites with varying Si/Al ratios. This enabled us to illustrate the importance of the extraframework sodium cations to the interaction with organometallic adsorbents in the supercages. Furthermore, changes in the conformation of the cobalt complex have been monitored by static, variable temperature ^{13}C NMR measurements on $Co(C_5H_5)(CO)_2$ which was enriched with ^{13}C at the CO ligands.

Experimental Section

Sample Preparation. The synthetic faujasite-type zeolite series NaY/NaX was obtained from Akzo Nobel Chemicals. The unit cell compositions of these materials in dehydrated notation are $Na_{89}(AlO_2)_{89}(SiO_2)_{103}$, $Na_{78}(AlO_2)_{78}(SiO_2)_{114}$, $Na_{62}(AlO_2)_{62}(SiO_2)_{130}$, $Na_{55}(AlO_2)_{55}(SiO_2)_{137}$, and $Na_{46}(AlO_2)_{46}(SiO_2)_{146}$, respectively. Dehydration was typically carried out as follows: Ca. 1 g of zeolite powder was filled into glass ampules forming a bed of approximately 4 cm in height. Subsequently, the bed was evacuated at room temperature overnight, then warmed to 323 K at 1 K min^{-1}, held at this temperature for 2 h, and finally heated to 723 K at 3 K min^{-1}. The temperature was maintained at this level for 5 h. The whole procedure was carried out while continuously pulling vacuum. After the ampules had been cooled to room temperature, they were flame sealed under vacuum and stored until use.

Loading experiments with $Fe(C_5H_5)_2$ were carried out in a nitrogen atmosphere in a glovebox. Dehydrated zeolite powder and freshly sublimed $Fe(C_5H_5)_2$ were combined gravimetrically in a mortar, mixed by crushing the two components, and then poured into an ampule which was sealed under vacuum and heated overnight at 373 K. The number of $Fe(C_5H_5)_2$ molecules per supercage is indicated by the designation xFe$(C_5H_5)_2$/$Na_{55}Y$.

Red-brown, liquid $Co(C_5H_5)(CO)_2$ was loaded into dehydrated NaY by evaporating a stoichiometric amount of the liquid under vacuum and contacting the vapor with the zeolite powder which was present in an ampule. Subsequently, the ampule was sealed and heated overnight at 373 K. In this way, two different loadings of NaY were prepared. The enrichment of $Co(C_5H_5)(CO)_2$ in ^{13}C nuclei was carried out in the zeolite. In a glovebox, NaY, loaded with the cobalt complex, was brought in an ampule and subsequently evacuated at 343 K for 15 min. During this treatment the sample turned green, indicating a partial decarbonylation of the cobalt complex.[9] Then the sample was contacted with labeled ^{13}CO gas (Campro Scientific, 99.3% ^{13}C) at atmospheric pressure, which led to an immediate color change from green to the original yellowish brown. This procedure was repeated three times, followed by a final evacuation at room temperature. Then the ampule was flame sealed while the sample was kept at liquid nitrogen temperature. About 75% of the CO ligands were labeled as estimated from the intensities of the peaks in the ^{13}C NMR spectrum which represent the carbon atoms of the cyclopentadienyl ring and the carbonyl ligands.

For the ^2H NMR experiments, deuterated $Fe(C_5D_5)_2$ was prepared according to the following procedure: Perdeuterated cyclopentadiene, C_5D_6, was prepared by the method of Lambert and Finzel[36] and was reacted with sodium wire in tetrahydrofuran (THF) to give NaC_5D_5. In the following step, perdeuterated $Fe(C_5D_5)_2$ was prepared by reacting NaC_5D_5 with anhydrous $Fe(II)Cl_2$ in THF and recrystallized from petroleum ether (40−60 °C).[37] These reactions were carried out under a nitrogen atmosphere by use of standard Schlenk techniques. From ^1H NMR measurements it was determined that $Fe(C_5D_5)_2$ was deuterated >99%. Prior to the loading experiments perdeuterated $Fe(C_5D_5)_2$ was freshly sublimed.

For the Mössbauer experiments ^{57}Fe-enriched $Fe(C_5H_5)_2$ was prepared. 50 mg ^{57}Fe and 50 mg naturally abundant iron were reacted with Cl_2 gas by a method described by Bauer[38] to give anhydrous $Fe(III)Cl_3$. According to Jolly,[39] anhydrous $Fe(III)Cl_3$ can be used instead of $Fe(II)Cl_2$ in the synthesis of $Fe(C_5H_5)_2$ although a somewhat lower yield is to be expected. $Fe(III)Cl_3$ was then reacted with NaC_5H_5 in THF in a similar manner as described above to yield 50% ^{57}Fe-enriched $Fe(C_5H_5)_2$. Purification of the sample was performed by sublimation of $Fe(C_5H_5)_2$.

Characterization. *NMR Experiments.* All solid-state NMR spectra on stationary samples were recorded on a Bruker MSL-400 spectrometer operating at a magnetic field of $B_0 = 9.4$ T. Chemical shifts are reported relative to tetramethylsilane (^{13}C) and deuterated water (^2H). Nonspinning $\{^1H\text{-}\}^{13}C$ CP NMR experiments were carried out with a standard Bruker 7 mm MAS probe head. Spinning was prevented mechanically by putting a second rotor on top of the sample rotor. A single contact spin-lock CP sequence was applied. Matching conditions, contact times, and recycle delays were empirically adjusted to maximum signal intensity. Contact times in the range of 1−10 ms and recycle delays of 2 s were typical. A decoupling field of 40 kHz has been used. Static ^2H quad-echo and ^{13}C Hahn-echo NMR experiments were obtained by use of a static probe head in sealed glass ampules of 1 cm diameter. The ^2H quad-echo NMR spectra were obtained by application of the quadrupole echo technique ($\pi/2_x$-τ-$\pi/2_y$-τ-acquire) with $\pi/2$ pulse lengths of 7 μs and recycle delays of 2 s. The influence of the pulse length used on the line shape has been checked by measuring the ^2H NMR spectrum of polycrystalline $Fe(C_5D_5)_2$, which is known. No distortion of the line shape by the relatively long pulse was observed. Typically, 500 scans were sufficient to obtain a good signal-to-noise ratio. ^{13}C NMR data were acquired using a Hahn-echo sequence ($\pi/2$-τ-π-acquire) with $\pi/2$ pulse lengths of 9.9 μs and recycle delays of 5 s. Variable temperature ^{13}C MAS spectra were recorded on a Bruker AM-500 spectrometer using a homemade probe head. Spinning speeds varied between 1.5 and 3.5 kHz. The spectra were analyzed using the Bruker software WINNMR and WINFIT.

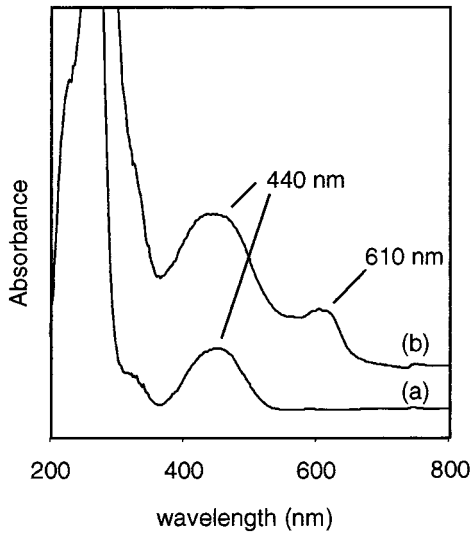

Figure 2. DREAS spectra of (a) $2Fe(C_5H_5)_2/Na_{55}Y$ and (b) $2Fe(C_5H_5)_2/Na_{55}Y$, after 1 h of exposure to air.

Other Techniques. ^{57}Fe Mössbauer measurements were made by use of a constant acceleration type instrument. The spectra were least-squares fit to Lorentzian line shapes. Mössbauer data were obtained at 13 different temperatures between 77 and 473 K for ^{57}Fe-enriched $1Fe(C_5H_5)_2/Na_{55}Y$. The series was started at 303 K followed by measurements at increased temperatures, i.e., 323, 348, 373, 398, 423, and 448 K. Then the temperature was reduced to 303 K, at which point an additional spectrum was measured. A further decrease of the temperature was carried out while taking spectra at 273, 223, 173, 123, and 77 K. Subsequently, the temperature was raised to 473 K. After recording a Mössbauer spectrum at this temperature, the temperature was lowered to 303 K, at which temperature a final control spectrum was measured.

Diffuse reflectance electronic absorption spectroscopy (DREAS) measurements were performed on a Hitachi 150-20 spectrophotometer equipped with a diffuse reflectance unit. After baseline correction, the reflectance spectra are converted to absorption spectra by application of the Kubelka−Munk function.

Results

Ferrocene in $Na_{55}Y$. In contrast to what has been reported earlier by Ozin et al.[32] and Suib et al.,[33] no oxidation under anaerobic conditions of intrazeolite $Fe(C_5H_5)_2$ to ferrocenium ions, $[Fe(C_5H_5)_2]^+$, has been observed, either by DREAS (see Figure 2a), or by Mössbauer spectroscopy. Different experimental conditions are likely to be responsible for this discrepancy in observations. Suib et al. found a second signal in their Mössbauer spectra which they assigned to the presence of ferrocenium ions in the material. However, in contrast to the experiments described here they did not dehydrate their samples thoroughly and mentioned themselves that water could be the cause for the oxidation of intrazeolite $Fe(C_5H_5)_2$. Ozin et al., on the other hand, carried out careful dehydrations of the zeolite samples, but used a different loading procedure based on liquid

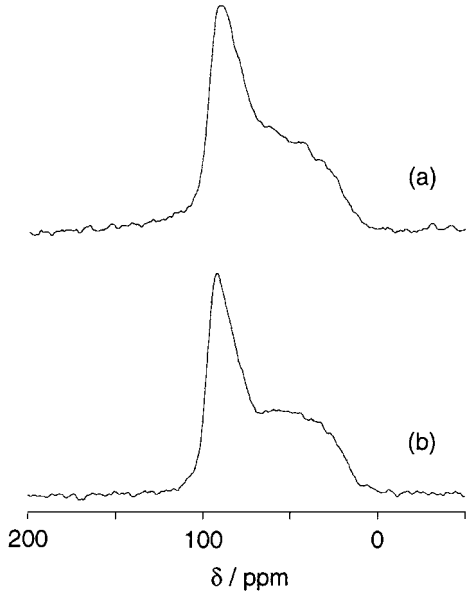

Figure 3. $\{^1H\text{-}\}^{13}C$ CP NMR spectra of (a) $2Fe(C_5H_5)_2/Na_{55}Y$, measured at 300 K, and (b) $2Fe(C_5H_5)_2/Na_{55}Y$, measured at 275 K. In both cases, a contact time of 1 ms was used.

phase absorption of $Fe(C_5H_5)_2$ from a pentane solution. Minor traces of water and/or oxygen in the solution could be the reason for the partial oxidation of intrazeolite $Fe(C_5H_5)_2$. We have observed that, in contrast to bulk $Fe(C_5H_5)_2$, intrazeolite $Fe(C_5H_5)_2$ is very sensitive to oxidation upon exposure to air. The DREAS spectra reveal that, in addition to the charge transfer band at ca. 440 nm, characteristic for $Fe(C_5H_5)_2$, a second charge transfer band is arising at 610 nm when the sample is contacted with air (see Figure 2b). This second band is typical for ferrocenium ions. Therefore, we attribute the oxidation of intrazeolite $Fe(C_5H_5)_2$ to the presence of water and/or oxygen in the sample.

The $\{^1H\text{-}\}^{13}C$ CP NMR spectrum of $2Fe(C_5H_5)_2/Na_{55}Y$ taken at 300 K is presented in Figure 3a. It consists of an axially symmetric powder pattern originating from magnetically equivalent ^{13}C atoms of the C_5H_5 rings. The line shape indicates that the molecular motion of the $Fe(C_5H_5)_2$ molecules is restricted to rapid rotation ($\tau_R^{-1} > 10^5$ Hz; τ_R is the correlation time of the rotational motion) of the cyclopentadienyl rings about their 5-fold axes. A static or slowly reorienting molecule (slow on the time scale of the NMR experiment; $\tau_R^{-1} < 10^3$ Hz) would result in an asymmetric powder pattern because of an asymmetry of the chemical shift tensor of the ^{13}C nuclei of the cyclopentadienyl rings.[40] Rapid rotation about a molecular axis causes a partial averaging of the chemical shift tensor, making it axially symmetric. Figure 3b shows a $\{^1H\text{-}\}^{13}C$ CP NMR spectrum taken from the same sample with identical acquisition parameters, however, measured at a somewhat lower temperature of 275 K. The line shape shows a loss in intensity at ca. 70 ppm as compared to that presented in Figure 3a and indicates that the $Fe(C_5H_5)_2$ molecules in the supercages of NaY are getting increasingly rigid. This is explained by the fact that cross-polarization is based on dipolar interaction between unlike spins which is strongly suppressed at the magic angle 54.74°.[41] This angle equals the position in the powder spectrum at

$$(\delta_{iso} - \delta_\perp)/(\delta_\parallel - \delta_\perp) = \frac{1}{3} \qquad (1)$$

$\delta_\perp$ represents the two averaged components of the chemical shift tensor, $\delta_\parallel$ is the chemical shift along the unique direction of

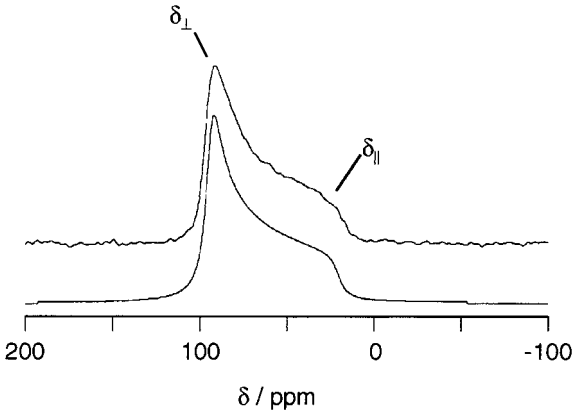

Figure 4. Experimental (upper trace) and simulated (lower trace) $\{^1H\text{-}\}^{13}C$ CP NMR spectrum of $2Fe(C_5H_5)_2/Na_{55}Y$, measured at 300 K.

the shift tensor. In the present study, $\delta_\perp = 98.0$ ppm and $\delta_\parallel = 20.1$ ppm, thus giving $\delta_{iso} = 72$ ppm, close to the observed minimum of 70 ppm. Because cross-polarization in these samples is expected to be almost entirely intramolecular, a slowing down of the molecular motion would mean that a number of $Fe(C_5H_5)_2$ molecules have their molecular axis at an angle of 54.74° with the magnetic field, B_0, and thus yield a less efficient cross-polarization as expressed by a reduction of the signal intensity at, in this case, ca. 70 ppm. By using longer contact times full cross-polarization was obtained. This situation is very similar to that obtained for solid benzene, which is known to rotate rapidly on the NMR time scale, described by Pines et al.[41] With short contact times, they observed a minimum in the powder pattern at δ_{iso}. No minimum was observed with longer contact times.

Figure 4 shows the experimental spectrum of $2Fe(C_5H_5)_2/Na_{55}Y$ taken at 300 K together with the simulation. The spectral parameters, $\delta_{iso} = 69.7$ ppm and span $\Omega = 75.0$ ppm, deviate only slightly from those reported in the literature,[42] $\delta_{iso} = 69.2$ ppm and $\Omega = 76$ ppm for polycrystalline $Fe(C_5H_5)_2$. This indicates that the nature of the $Fe(C_5H_5)_2$ molecules has not changed much upon absorption in the supercages of the zeolite. A similar observation was made upon analysis of the ^2H quad-echo NMR and Mössbauer spectra (see below).

The ^2H quad-echo NMR spectra measured as a function of temperature are presented in Figure 5. The line shape of the spectra changes considerably upon variation of the temperature. All spectra contain one signal caused by the magnetically equivalent ^2H nuclei attached to the C_5D_5 rings. At the lowest temperatures the line shape consists of a Pake-type powder pattern, characteristic for $I = 1$ nuclei under static conditions. The distance between the maxima of the Pake doublet, at high and low loading, is 73 kHz, leading to a quadrupole coupling constant, QCC, of 97.3 kHz. This is exactly the same value as we have measured for crystalline $Fe(C_5D_5)_2$ (not shown) and is about half that expected for a rigid ^2H-nucleus. According to:

$$QCC_{rot} = \frac{1}{2}(3\cos^2\theta - 1)QCC_{rigid} \qquad (2)$$

where θ is the angle between the C−D bond direction and the axis of rotation, this is consistent with rapid cyclopentadienyl ring rotation as the only dynamic averaging process affecting the electric field gradient tensor of the deuterons.

As the temperature increases, other types of motion start to affect the line shape of the spectra and this effect depends on the loading. At these intermediate temperatures the line shape

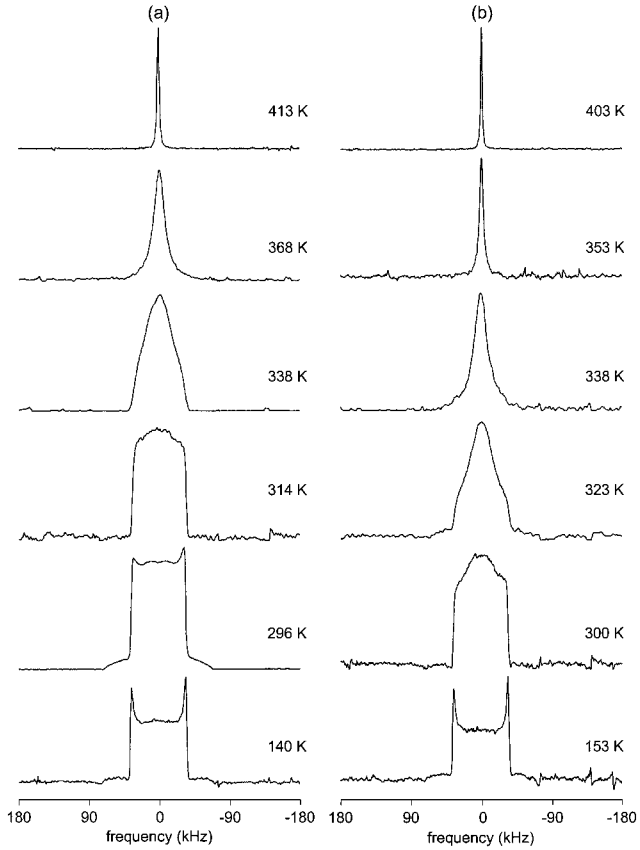

Figure 5. ^{2}H quad-echo NMR spectra of $Fe(C_5H_5)_2$ in zeolite $Na_{55}Y$ at the indicated temperatures. (a) Loading of two $Fe(C_5H_5)_2$ molecules per supercage. (b) Loading of one $Fe(C_5H_5)_2$ molecule per supercage.

changes as a function of the rate of the motions. Motion with a rate smaller than ca. 10^3 Hz is said to be in the "slow" regime and the line shape is not affected by the rate of motion. Motion of rate faster than ca. 10^8 Hz is said to be in the "fast" regime, and it means that a further increase of the rate of motion has no effect on the line shape. Between these two regimes the line shape does change as a function of the rate of motion, the "intermediate" regime. At temperatures above 353 K the line shape has changed to a Lorentzian-shaped line, which narrows on a further increase of the temperature. This line shape is indicative for isotropic motional behavior of the ferrocene molecules within the voids of the zeolite.

Representative spectra of the Mössbauer spectra of $1Fe(C_5H_5)_2/Na_{55}Y$ are shown in Figure 6. At first sight the spectra are composed of one doublet signal. When raising the temperature to 448 K, the line width of this doublet increases. Table 1 shows the Mössbauer parameters of this signal as a function of temperature for the first temperature slope from 303 to 448 K. The spectral parameters obtained at 303 K compare well with those measured for polycrystalline $Fe(C_5H_5)_2$ at the same temperature, which gave an isomer shift δ of 0.71 mm s^{-1} and a quadrupole splitting ΔE_Q of 2.38 mm s^{-1}. The spectrum taken at 448 K clearly shows an asymmetric shape of the doublet (see Figure 6). Because doublet signals in Mössbauer spectra of powdered samples are necessarily symmetric, the only physical explanations that can clarify the asymmetry are preferred orientation of the loaded zeolite crystals in the sample or the presence of an additional component. Preferred orientation is not likely because the crystallites of zeolite NaY are very small (ca. 10 μm). Moreover, if preferred orientation is the cause of the observed asymmetry, this would have been found at the

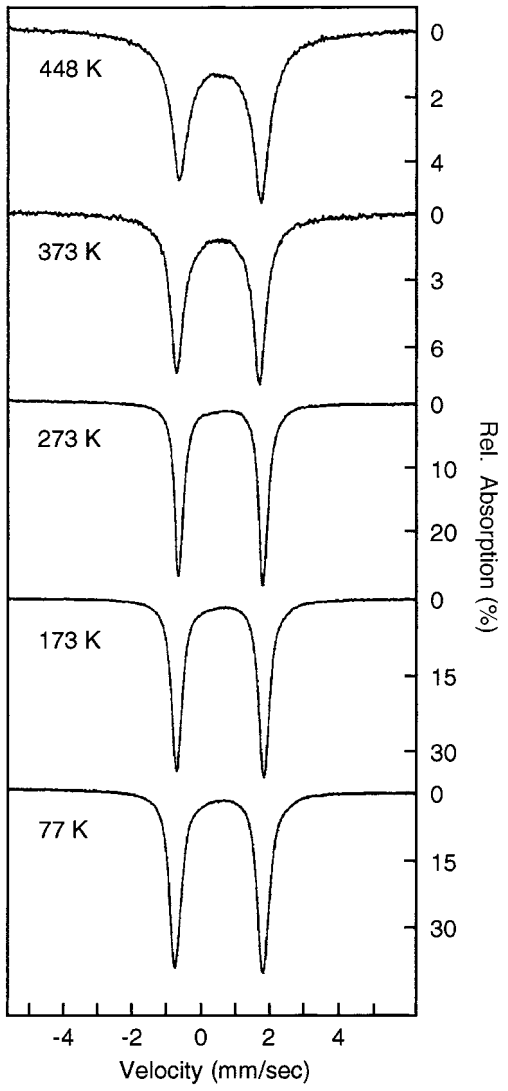

Figure 6. Mössbauer spectra of $1Fe(C_5H_5)_2/Na_{55}Y$ as a function of temperature.

TABLE 1: Mössbauer Fitting Parameters for $1Fe(C_5H_5)_2/Na_{55}Y$ at Temperatures between 303 and 448 K

T (K)	δ (mm s^{-1})	ΔE_Q (mm s^{-1})	Γ (mm s^{-1})
303	0.73	2.43	0.34
323	0.72	2.42	0.36
348	0.70	2.41	0.41
373	0.69	2.41	0.43
398	0.68	2.42	0.44
423	0.66	2.41	0.54
448	0.66	2.40	0.59

lowest temperatures as well. As this is not the case, the only possible explanation that remains is the presence of a contamination. The measurement at 77 K shows that this contamination is small because it is hardly visible in the Mössbauer spectrum. The reason that it has a higher intensity at elevated temperatures is explained by the fact that it has a higher Debye temperature, i.e., it is bonded more strongly to the zeolite lattice than the $Fe(C_5H_5)_2$ molecules. A comparison of the Mössbauer parameters of the spectrum taken at 77 K, i.e., $\delta = 0.800$ mm s^{-1} and $\Delta E_Q = 0.509$ mm s^{-1} with literature data on polycrystalline $Fe(C_5H_5)_2$ being $\delta = 0.78$ mm s^{-1} and $\Delta E_Q = 2.381$ taken at 87 K[43] shows small deviations which could be explained by host−guest interactions.

The second Mössbauer spectrum measured at 303 K, after a decrease in temperature from 448 K, revealed a remarkable

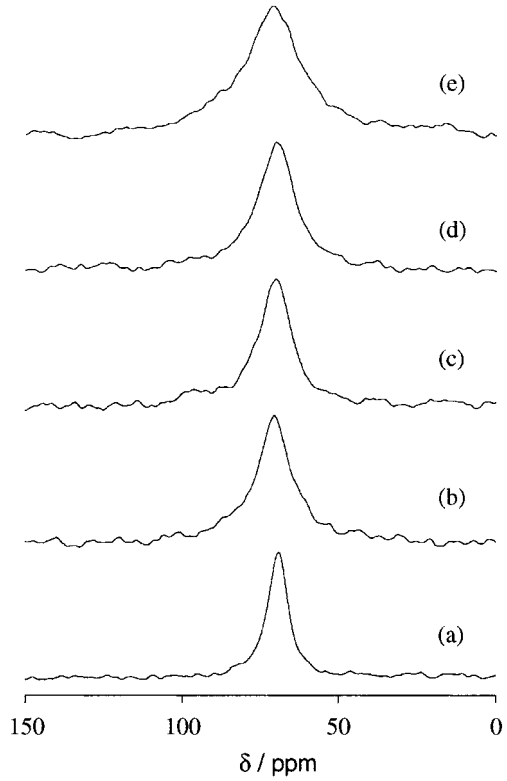

Figure 7. Static $\{^1H\text{-}\}^{13}C$ CP NMR spectra of $1Fe(C_5H_5)_2/Na_{55}Y$ as a function of Si/Al ratio: (a) Si/Al = 1.16, (b) Si/Al = 1.46, (c) Si/Al = 2.08, (d) Si/Al = 2.42, (e) Si/Al = 2.86.

increase in relative absorption area. Moreover, the line width of the main component has decreased somewhat compared to that observed for the same component at the start of the data series (Γ_{first} = 0.34 mm s^{-1}, Γ_{second} = 0. 30 mm s^{-1}). The increase in relative absorption area is related to the Debye temperature and means that the ferrocene molecules are getting more rigid. Moreover, the decrease in line width, which is related to the correlation time of motion, also indicates an increasing rigidity of the ferrocene molecules. After further decreasing the temperature to 77 K, the sample temperature was raised to 473 K. Now strong changes in the Mössbauer spectrum became apparent which on lowering the temperature to 303 K were clearly visible in the spectrum taken at this temperature (not shown). Because the reason for these chemically induced changes in the Mössbauer spectrum is not clear, no further attention has been paid to these effects.

Ferrocene in NaY(X) Zeolites with Varying Si/Al Ratios. Static $\{^1H\text{-}\}^{13}C$ CP NMR spectra of intrazeolite $Fe(C_5H_5)_2$ molecules have been measured and are presented in Figures 7 and 8. All spectra were obtained at room temperature. The width at half-height of the signals with a Lorentzian line shape obtained from $1Fe(C_5H_5)_2/NaY$ increases with increasing Si/Al ratio (see Table 2) and clearly indicates an increased motional averaging of the anisotropy at low Si/Al ratios. At full loading, i.e., $2Fe(C_5H_5)_2/NaY$, the effect of the composition of the faujasite-type zeolite on the molecular motion of the $Fe(C_5H_5)_2$ molecules is less pronounced. All spectra reveal an axially symmetric powder pattern, which means that the only motional process affecting the NMR line shape is rapid rotation ($>10^6$ s^{-1}) of the cyclopentadienyl rings. However, the powder patterns of the samples with the lowest (Si/Al = 1.16) and highest (Si/Al = 3.14) silicon ratio show some disorder, indicating that other motions are affecting the line shape as well.

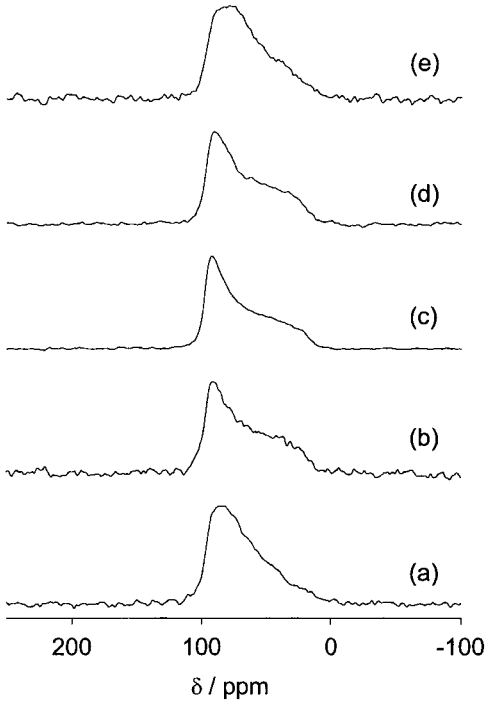

Figure 8. Static $\{^1H\text{-}\}^{13}C$ CP NMR spectra of $2Fe(C_5H_5)_2/Na_{55}Y$ as a function of Si/Al ratio: (a) Si/Al = 1.16, (b) Si/Al = 1.46, (c) Si/Al = 2.08, (d) Si/Al = 2.42, (e) Si/Al = 3.14.

TABLE 2: Width at Half Height, $\Delta\omega_{1/2}$, of ^{13}C Signal in $\{^1H\text{-}\}^{13}C$ CP NMR Spectra as a Function of Si/Al Ratio

Si/Al ratio	$\Delta\omega_{1/2}$ (Hz)
1.16	767
1.46	1425
2.08	1360
2.42	1481
2.86	2353

Dicarbonylcyclopentadienylcobalt in $Na_{55}Y$. The room temperature $\{^1H\text{-}\}^{13}C$ CP NMR spectrum of NaY loaded with $Co(C_5H_5)(CO)_2$ (not shown) reveals one signal with a Gaussian line shape at δ_{iso} = 86.5 ppm, which originates from the ^{13}C nuclei of the cyclopentadienyl ring. The chemical shift is in good agreement with the chemical shift observed in solution, 84.5 ppm in $CDCl_3$.[44] Because of the large distance between the ^1H nuclei of the cyclopentadienyl ring and the ^{13}C nuclei of the CO ligands, signal enhancement of the latter carbon atoms by cross-polarization is relatively weak and thus these signals are not observed. Upon decreasing the temperature from 263 to 183 K the spectra change considerably (see Figure 9). At 263 K a peak with a Gaussian line shape is observed which is assigned to isotropic motion of the cyclopentadienyl ring, while at temperatures below 203 K an axially symmetric powder pattern becomes visible. This line shape is indicative of a limitation of the motional freedom of the $Co(C_5H_5)(CO)_2$ molecules to anisotropic rotation of the cyclopentadienyl ring about the 5-fold axis. Additionally, it is observed that the appearance of the broad line follows nearly the same temperature dependence for a loading of one and two molecules per supercage. The parameters belonging to the powder pattern are given as δ_{iso} = 86.5 ppm and Ω = 92.3 ppm.

After enrichment of the CO ligands in ^{13}C, it proved possible to examine the carbonyl signal in the ^{13}C Hahn-echo NMR spectrum as a function of temperature (see Figure 10a). The spectra presented here are taken from a sample with a loading of one molecule $Co(C_5H_5)(CO)_2$ per supercage. Similar results were obtained at full loading (two molecules per supercage).

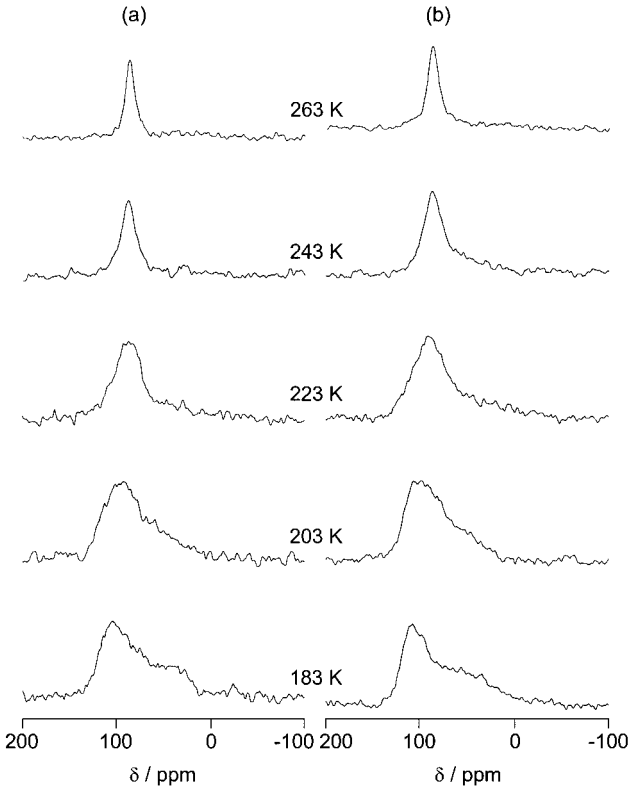

Figure 9. $\{^1H\text{-}\}^{13}C$ CP NMR spectra of $Co(C_5H_5)(CO)_2$ in zeolite $Na_{55}Y$ at (a) half loading of one molecule per supercage and (b) full loading (two molecules per supercage). The temperatures at which the spectra were measured are indicated in the figure.

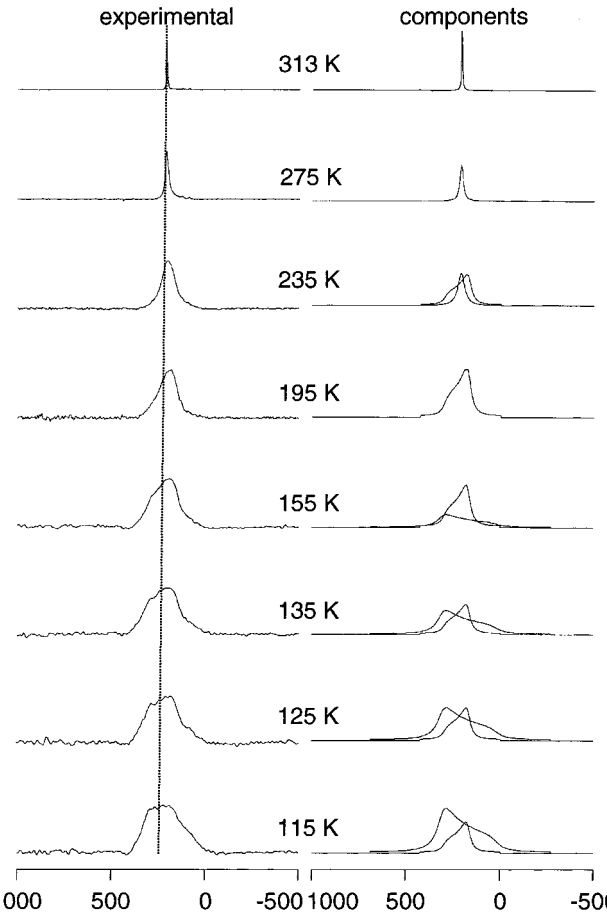

Figure 10. Experimental (left) and simulated (right) ^{13}C Hahn-echo NMR spectra of $Co(C_5H_5)(CO)_2$ in $Na_{55}Y$ at a loading of one molecule per supercage. The temperatures are indicated in the figure. The dotted line marks the isotropic chemical shift δ_{iso} at 209 ppm.

At 313 K the spectrum consists of a single narrow Gaussian line at 209 ppm, which is caused by the ^{13}C nuclei of the carbonyl ligands (δ = 205 ppm in $CDCl_3$,[44]). When the temperature is decreased, the component at 209 ppm starts to broaden and at 235 K an asymmetric line shape becomes apparent which is followed by a shift of the highest intensity in the spectrum to lower frequencies at 195 K. Upon a further decrease of the temperature, a shoulder appears at the left-hand side in the spectrum which increases in intensity at lowering the temperature further to 115 K. These spectra are deconvoluted as shown in Figure 10. At the highest temperatures of 313 and 275 K, the spectrum consists of a single Gaussian component. At 235 K the spectrum is composed of this Gaussian component and an axially symmetric powder pattern with a span Ω of 127 ppm and δ_{iso} = 209 ppm. On decreasing the temperature to 195 K the intensity of the broad component grows at the expense of the Gaussian line. At 155 K the Gaussian line has disappeared completely, and an additional chemical shift powder pattern is observed with δ_{iso} = 209 ppm and Ω = 287 ppm. This powder pattern is inverted compared to the narrower powder pattern. On a further decrease of the temperature, this component increases in intensity at the cost of the smaller powder pattern.

Discussion

The NMR experiments show that, at low temperatures, $Fe(C_5H_5)_2$ in $Na_{55}Y$ adsorbs to the zeolite lattice in such a way that its motional freedom is restricted to rapid rotation of the cyclopentadienyl rings. As the temperature is raised the molecules undergo some kind of orientational randomization which affects the NMR line shapes but not the Mössbauer line shapes. The Mössbauer data suggest that the randomization involves translational processes rather than reorientation of the molecular principal axis. Reorientations of this type include rapid reorientation of the molecular axis in a plane or isotropic reorientation of the molecular axis. In the former case this would give a doublet in the Mössbauer spectrum with reduced quadrupole splitting, while the latter would give rise to a singlet.[45] None of these line shapes were observed in the Mössbauer spectra. Instead, a strong decrease in relative absorption area and an increase in line width at higher temperatures was found, which can only be explained by the fact that the $Fe(C_5H_5)_2$ molecules gain increasing translational freedom in the voids of the zeolite.[46] The relative absorption area of the Mössbauer spectrum taken at 303 K increased in combination with a decrease in line width after taking a series of measurements at elevated temperatures compared to the values found before these heat treatments. This suggests that the $Fe(C_5H_5)_2$ molecules, or part of the molecules, get increasingly rigid. One explanation could be that the molecules stick more strongly to the zeolite lattice after this heat treatment. More likely is the explanation that after prolonged heat treatment (data acquisition for one Mössbauer spectrum takes ca. 10 h.) part of the $Fe(C_5H_5)_2$ molecules diffuse out of the zeolite pores and form small crystallites at the outer surface of the porous material. It was observed on previous not-enriched samples that after long measuring times at temperatures above 473 K orange crystallites of $Fe(C_5H_5)_2$ were formed at the exterior of the pressed sample. Moreover, the Mössbauer spectrum of polycrystalline $Fe(C_5H_5)_2$ shows narrow lines with a width of 0.250 mm s^{-1}, which is indicative for an increased rigidity of the ferrocene molecules

in its crystalline matrix as compared to ferrocene molecules in the voids of zeolite NaY. This effect would have only a very small influence on the NMR spectra since the measuring times were much shorter (e.g., 15 min for obtaining a ^{2}H quad-echo NMR spectrum) as well as the measuring temperature, which did not go over 413 K.

It is also deduced from the Mössbauer data that the interaction between the zeolite lattice and $Fe(C_5H_5)_2$ molecules does not proceed by the iron atom of the organometallic. The data show that the changes in electric field gradient (EFG) tensor are small, indicating that it is predominantly molecular in origin with little contribution from the zeolite lattice. The iron atom in $Fe(C_5H_5)_2$ is not reactive, although, weak, protonated species have been obtained. These compounds give strong changes in the Mössbauer spectrum as compared to crystalline $Fe(C_5H_5)_2$.[47] This observation cancels out the possibility of a sodium−iron interaction, as a kind of Lewis acid−Lewis base interaction. Therefore, it is concluded that the interaction between the zeolite host and $Fe(C_5H_5)_2$ guest involves the aromatic cyclopentadienyl rings of the $Fe(C_5H_5)_2$ molecules. This conclusion is supported by studies carried out on benzene, C_6H_6, in NaY and NaX.[10,13,48−52] In order to set up a model to describe the dynamic behavior of $Fe(C_5H_5)_2$ in NaY it is instructive to take a closer look at these systems first.

It was shown by Fitch et al.[13] that, at low temperatures, C_6H_6 has two adsorption sites in NaY (Si/Al = 2.43). One dominant site is located in the supercage with the benzene molecule facially coordinated to the sodium cation at the SII position, the other site, which is expected to be occupied only at higher loadings, is centered in the 12-ring window. Modeling studies of the dynamics of C_6H_6 in NaY[50] revealed that SII→SII jumps are the major cause of orientational randomization of these molecules (SII→SII, E_A = 35 kJ mol^{-1}). *Inter*cage migration, which can only proceed by a jump of the C_6H_6 molecule from a SII site to a 12-ring window followed by a jump to a SII site in an adjacent supercage, is less favorable because of a higher energy barrier of the SII-to-window (W) jump (SII→W, E_A = 41 kJ mol^{-1}).

A powder neutron diffraction study of C_6H_6 in zeolite NaX (Si/Al = 1.2)[52] located half of the benzene molecules in a similar position coordinated to sodium cations at the SII position as was found for C_6H_6 in NaY, but in contrast to that system, no C_6H_6 could be found in the 12-ring window. It was argued that sodium ions at the SIII sites prevent C_6H_6 from occupying that position. Auerbach et al.[51] earlier showed by using kinetic Monte Carlo methods that an increase of Na^+ cations in the supercages leads to a higher mobility of the C_6H_6 molecules in NaX as compared to NaY. Second, it was observed that the relative magnitudes of *intra*cage and *inter*cage hopping are of equal size, meaning that both processes contribute to the same extent to orientational randomization of the C_6H_6 molecules.

Similarly to the systems described above, $Fe(C_5H_5)_2$ molecules get increasingly mobile when the zeolite host is changed from NaY to NaX. It supports the idea that the interaction between zeolite and $Fe(C_5H_5)_2$ takes place via the extraframework Na^+ ions and aromatic cyclopentadienyl ligands. In addition to what has been found for benzene in NaY, we think that the 12-ring window is an even less favorable adsorption site for the $Fe(C_5H_5)_2$ molecules, because of the smaller size and the 5-fold symmetry of the cyclopentadienyl ligands. This would reduce the stabilization of 12-ring window site by the framework oxygen atoms of the zeolite considerably as compared to C_6H_6 where the 12 oxygen atoms of the window provide a close-fitting environment.[13] These assumptions would

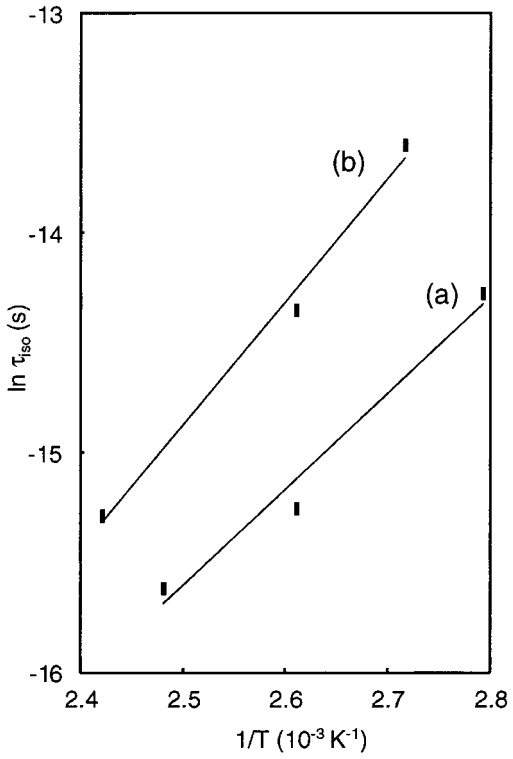

Figure 11. Temperature dependence of the correlation time for isotropic reorientation, τ_{iso}, for (a) $1Fe(C_5H_5)_2/Na_{55}Y$ and (b) $2Fe(C_5H_5)_2/Na_{55}Y$.

imply that, for $Fe(C_5H_5)_2$ in NaY, orientational randomization is predominantly caused by *intra*cage diffusion processes. Moreover, it is likely that *inter*cage diffusion is not only hindered by a less favorable absorption to the 12-ring window site, but also by the geometry of the $Fe(C_5H_5)_2$ molecule, with its two cyclopentadienyl rings, which makes cage-to-cage diffusion through the 12-ring window much more difficult than for the flat benzene molecules.

If we assume that, on the basis of the arguments mentioned before, *intra*cage diffusion is the main process of reorientational randomization of the $Fe(C_5H_5)_2$ molecules a correlation time, τ_{iso}, can be derived from the line width at half-height, $\Delta\nu_{1/2}$, of the Lorentzian lines found in the ^{2}H NMR spectra at the highest temperatures according to:[53]

$$\Delta\nu_{1/2} = \frac{9\pi}{20}(QCC_{rot})^2\tau_{iso} \qquad (3)$$

under the constraint $\tau_{iso} \gg \omega_L^{-1}$ (ω_L is the Larmor frequency). If we assume that in this limited temperature regime (358−413 K) *intra*cage isotropic translational reorientation is the only motional process affecting the ^{2}H quad-echo NMR line shape, a plot of τ_{iso} against the inverse of the temperature (see Figure 11) gives activation energies, E_A, for the isotropic motion of the $Fe(C_5H_5)_2$ molecules in the supercages of NaY according to the Arrhenius-type expression:

$$\tau_{iso} = \tau_{iso(0)} \exp(E_A/RT) \qquad (4)$$

This leads to activation energies, E_A, of 36.2 and 46.4 kJ mol^{-1} for $1Fe(C_5H_5)_2/Na_{55}Y$ and $2Fe(C_5H_5)_2/Na_{55}Y$, respectively. These activation energies can then be identified as energy barriers for SII→SII jumps. The difference in activation energy between the high-loaded sample and low-loaded sample, however, cannot be explained by the fact that *intra*cage motion

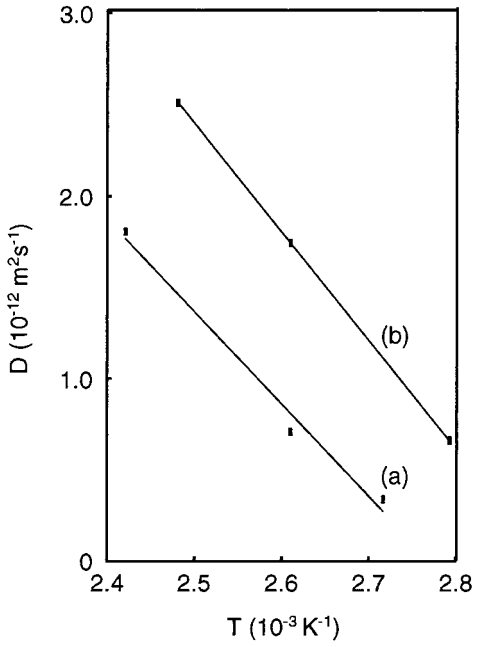

Figure 12. Intracrystalline diffusivities of (a) $2Fe(C_5H_5)_2/Na_{55}Y$ and (b) $1Fe(C_5H_5)_2/Na_{55}Y$ as determined from the line width, $\Delta\nu_{1/2}$, of the ^2H quad-echo NMR spectra.

requires a collective motion of both $Fe(C_5H_5)_2$ molecules in the supercage in case of full loading. Rather, $Fe(C_5H_5)_2$ adsorbs in different manners for half and full loading. An explanation could be that at half loading $Fe(C_5H_5)_2$ adsorbs with only one cyclopentadienyl ring to an SII site, with its molecular axis perpendicular to the plane of the six-ring of the SII site. This adsorption mode is similar to that found for benzene at the SII site.[13] At full loading, however, this adsorption mode is sterically hindered and therefore a change is expected to an adsorption mode where both cyclopentadienyl rings interact with two sodium cations on adjacent SII sites in a supercage. The fact that the activation energy for this adsorption mode is not twice that of the proposed adsorption mode at half loading could be explained by the difference in distance between Na^+ and the center of the C_5H_5 ring. At full loading the minimal distance between these interacting elements is 3.3 Å, while at half loading the distance between Na^+ and the C_5H_5 ring can be optimal because there is no competition between adsorption sites. For comparison, the distance between the sodium ion at the SII site and an adsorbed C_6H_6 molecule is 2.7 Å.[13]

Intracrystalline diffusivities can be obtained from the following expression,[10]

$$D = \frac{\langle l^2 \rangle}{6\tau_{iso}} \tag{5}$$

where $\langle l^2 \rangle$ is the mean square displacement per elementary site exchange jump. Here, we set, as an estimate, $\langle l^2 \rangle^{1/2}$ equal to 5 Å, which is the distance between two SII centers in a supercage minus twice the length of the sodium$-C_5H_5$ distance, which we have set to 3.3 Å. The intracrystalline diffusivities of $Fe(C_5H_5)_2$ in $Na_{55}Y$ are presented in Figure 12. It should be noted that these values represent *intra*cage diffusion only. Diffusivities obtained by other methods, such as pulsed field gradient NMR, could be completely different because they measure diffusion on a macroscopic scale, so as to obtain *inter*cage diffusion coefficients.

All translational motions of $Co(C_5H_5)(CO)_2$ in $Na_{55}Y$ are slow on the time scale of the $\{^1H\text{-}\}^{13}C$ CP NMR experiment at 183 K. At this temperature the line shape of the signal from the cyclopentadienyl ring clearly indicates anisotropic ring rotation as the dominant type of motion. This means that the line widths of the signals of ^{13}C nuclei belonging to the carbonyl ligands in the ^{13}C Hahn-echo NMR spectra contain information about the OC$-$Co$-$CO bite angle, φ. At this temperature and below, the only possible types of motion of the carbonyl ligands are free rotational diffusion or jumps about the 2-fold axis.

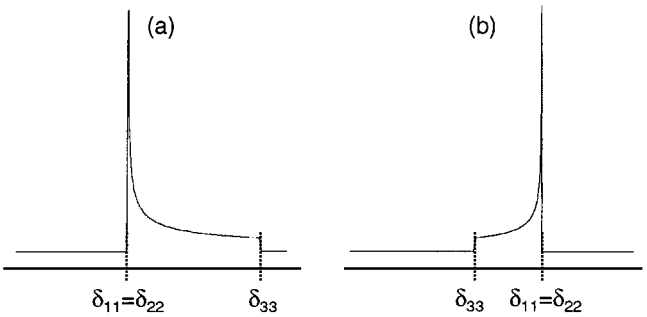

Figure 13. Examples of (a) axially symmetric powder pattern and (b) axially symmetric powder pattern inverted by motional averaging (see text).

In the case of free rotational diffusion, motional averaging of the shielding tensor, δ, is easily described. Because the shielding tensor is axially symmetric for ^{13}C nuclei of carbonyl ligands, the line width of the axially symmetric powder pattern in the fast motional limit observed in the ^{13}C Hahn-echo NMR spectrum is related to the angle between the CO bond direction and the rotation axis according to:

$$\Omega_{av} = \frac{1}{2}(3\cos^2 \alpha - 1)\Omega_{stat} \tag{6}$$

where Ω_{av} is the motionally averaged span, Ω_{stat} is the span for static carbonyl ligands, and α is the angle between CO bond direction and rotation axis. It is easily seen that for $\alpha = 54.74°$ (the magic angle) the chemical shift anisotropy is completely averaged and a sharp line is observed. For values higher than the magic angle an inverted chemical shift powder pattern is obtained (see Figure 13). The span of the inverted, motionally averaged powder pattern maximally reaches half the width of the static pattern ($\alpha = 90°$). In rationalizing the ^{13}C Hahn-echo NMR spectra of enriched $Co(C_5H_5)(^{13}CO)_2$ in zeolite NaY we have obtained a component with an inverted powder pattern (see Figure 10). This implies that in the case of free diffusional rotation, $Co(C_5H_5)(CO)_2$ molecules are present in the supercages of zeolite NaY with a OC$-$Co$-$CO bite angle, $\varphi > 109.5°$. Considering the OC$-$Co$-$CO bite angle of 98.4° obtained for $Co(C_5H_5)(CO)_2$ in the gas phase,[31] this means that the conformation of the cobalt complex changes significantly upon insertion in the zeolite. The second component with $\Omega = 287$ ppm and $\delta_{iso} = 209$ ppm cannot be easily explained (see Figure 10). It could be caused by stationary molecules or by molecules rapidly rotating about the 2-fold axis whose bite angle is smaller than twice the magic angle. A span of 287 ppm for stationary carbonyl ligands in $Co(C_5H_5)(CO)_2$ is unlikely. Common values for terminally bound CO ligands in metal carbonyl and "half-sandwich" carbonylcyclopentadienyl complexes are found in the range of 380 ± 60 ppm.[54,55] Thus, the observed span could be motionally averaged by molecules rotating freely about the 2-fold axis but with a different bite angle than those causing the inverted powder pattern. Until now, the principle values of the shielding tensor for ^{13}C nuclei of the CO ligands belonging to $Co(C_5H_5)(CO)_2$ are not known. This means that exact bite

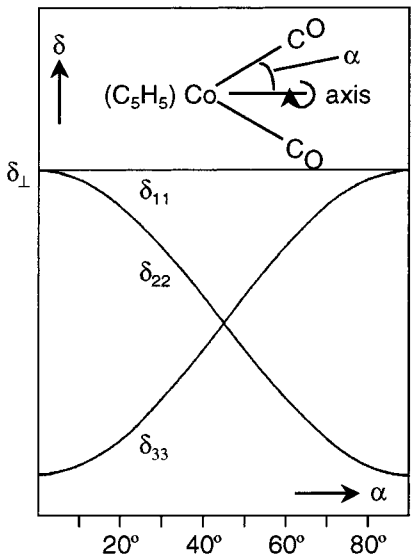

Figure 14. Effective principle components, δ, for a nucleus jumping rapidly between two sites, here illustrated for the carbonyl ligands in $Co(C_5H_5)(CO)_2$. The chemical shift tensors of both ^{13}C nuclei are axially symmetric.

angles cannot be given. However, if the span of stationary carbonyls in $Co(C_5H_5)(CO)_2$ is estimated at 440 ppm (based on $Fe(C_5H_5)_2(CO)_4$; $\Omega_{stat} = 444$ ppm and $CrCp(CO)_3$; $\Omega_{stat} = 431$ ppm), this would lead to bite angles of ca. 60° and 135°.

Jump rotations about a 2-fold axis lead to different line shapes than a motional process that is determined by free rotational diffusion about a 2-fold axis. In contrast to the static tensor, the motionally averaged chemical shift tensor, δ_{av}, is not necessarily axially symmetric. Only when the angle α between carbonyl ligand and the 2-fold rotation axis is 0°, 45°, or 90° is an axially symmetric powder pattern obtained; in all other cases the line shape consists of an asymmetric powder pattern. This is illustrated in Figure 14 which shows the course of the three principle components, δ_{11}, δ_{22}, and δ_{33} of the averaged chemical shift tensor δ_{av} as a function of the angle α. Because the experimental spectra have been rationalized by the presence of two axially symmetric powder patterns and one Gaussian line (see Figure 10), it is unlikely that the CO groups of the $Co(C_5H_5)(CO)_2$ molecules undergo jump rotations about the 2-fold axis. Assuming a jump model implies that the inverted component with chemical shift parameters $\delta_{iso} = 209$ ppm and $\Omega = 127$ ppm can only be explained by a bite angle of 90° (the bite angle φ is twice the angle α between CO ligand and rotation axis). This means that the span, Ω, for stationary CO ligands is twice that of the inverted component, which would be 254 ppm, a value which is highly unlikely for stationary CO ligands of transition metal carbonyl and half-sandwich complexes. Moreover, the other component with a span of 287 ppm would be the result of stationary $Co(C_5H_5)(CO)_2$ molecules or molecules rapidly rotating about the 2-fold axis with a bite angle of 180°. Again, this value falls out of the range commonly found for ^{13}C nuclei of carbonyl ligands. Therefore, we argue that free rotational diffusion is the type of process that determines the line shape of the ^{13}C signal of the carbonyl ligands.

Conclusions

It has been shown by static NMR techniques and by Mössbauer spectroscopy that the molecular motion of $Fe(C_5H_5)_2$ molecules in the voids of Na^+-containing faujasites can be described in some detail. At temperatures below 225 K it is confirmed by both ^2H quad-echo NMR and $\{^1H\text{-}\}^{13}C$ CP NMR spectroscopy that the $Fe(C_5H_5)_2$ molecules in $Na_{55}Y$ are firmly fixed in the zeolite, their only motional freedom being rapid rotation of the cyclopentadienyl rings about the 5-fold axis. As has been shown by Mössbauer spectroscopy, motional reorientations at higher temperatures involve translational processes rather than rotational reorientations. On the basis of these findings, a model was proposed for the translational randomization of intrazeolite $Fe(C_5H_5)_2$, under the assumption that *intra*cage site-to-site hopping is dominating over cage-to-cage hopping. From this, activation energies, E_A, and diffusion constants, D, have been calculated.

Room temperature $\{^1H\text{-}\}^{13}C$ CP NMR studies on faujasites with varying Si/Al ratios show an increase in molecular motion of the incorporated $Fe(C_5H_5)_2$ molecules at lower Si/Al ratios, the effect being related to the amount of $Fe(C_5H_5)_2$ present in the supercage. The higher number of sodium ions needed for charge compensation in NaX populate the SIII cation sites in the supercage and probably cause a decrease in activation energy for *intra*cage site-to-site hopping, such as SII→SIII jumps, similar to what has been observed for C_6H_6 in NaX.[10,51]

It has been shown by $\{^1H\text{-}\}^{13}C$ CP NMR that $Co(C_5H_5)(CO)_2$ at ambient temperature is highly mobile in the supercages of zeolite $Na_{55}Y$ but on a decrease of the temperature to 183 K gets bonded to adsorption sites in the zeolite. Variable temperature ^{13}C Hahn-echo NMR experiments on enriched $Co(C_5H_5)(^{13}CO)_2$ in zeolite $Na_{55}Y$ reveal conformational changes of the molecules. The inverted axially symmetric powder pattern unmistakably shows that the bite angle φ has changed for part of the intrazeolite $Co(C_5H_5)(CO)_2$ molecules from 98.4° for molecules in the gas phase to a value larger than 109.5°. This conclusion is based on the assumption that the CO ligands rotate freely about the 2-fold axis and do not undergo jump processes. A second axially symmetric powder pattern with a span of 287 ppm, which becomes visible at 155 K and below, points at the presence of intrazeolite $Co(C_5H_5)(CO)_2$ molecules with a bite angle smaller than 109.5°. From an estimated span of 440 ppm for static CO ligands in $Co(C_5H_5)(CO)_2$ molecules, bite angles of ca. 135° and 60° are obtained, respectively. The observation of two separate components in the ^{13}C Hahn-echo spectra of $Co(C_5H_5)(CO)_2$ supports the conclusion by Li et al.[30] that two adsorption modes are present in zeolite NaY.

References and Notes

(1) Ozin, G. A.; Gil, C. *Chem. Rev.* **1989**, *89*, 1749.
(2) Sachtler, W. M. H.; Zhang, Z. *Adv. Catal.* **1993**, *39*, 129.
(3) Bein, T. *Comprehensive Supramolecular Chemistry* 1st ed.; Atwood J. L., Davies, J. E. D., MacNicol, D. D., Vögtle, F., Eds.: Elsevier Science Ltd., 1996; Vol. 7, Chapter 20.
(4) Van de Goor, G.; Freyhardt, C. C.; Behrens, P. *Z. Anorg. Allg. Chem.* **1995**, *621*, 311.
(5) Behrens, P.; Van de Goor, G.; Freyhardt, C. C. *Angew. Chem., Int. Ed. Engl.* **1995**, *34*, 2680.
(6) Balkus, K. J.; Gabrielov, A. G.; Shepelev, S. *Microporous Mater.* **1995**, *3*, 489.
(7) Van de Goor, G.; Lindlar, B.; Felsche, J.; Behrens, P. *J. Chem. Soc., Chem. Commun.* **1995**, 2559.
(8) Van de Goor, G.; Hoffmann, K.; Kallus, S.; Marlow, F.; Schüth, F.; Behrens, P. *Adv. Mater.* **1996**, *8*, 65.
(9) Freyhardt, C. C.; Tsapatis, M.; Lobo, R. F.; Balkus, K. J., Jr.; Davis, M. E. *Nature* **1996**, *381*, 295.
(10) Burmeister, R.; Schwarz, H.; Boddenberg, B. *Ber. Bunsen-Ges. Phys. Chem.* **1989**, *93*, 1309.
(11) Koller, H.; Overweg, A. R.; van Santen, R. A.; de Haan, J. W. *J. Phys. Chem.* **1997**, *101*, 1754.
(12) Vitale, G.; Mellot, C. F.; Bull, L. M.; Cheetham, A. K. *J. Phys. Chem. B* **1997**, *101*, 4559.
(13) Fitch, A. N.; Jobic, H.; Renouprez, A. *J. Phys. Chem.* **1986**, *90*, 1311.

(14) van Dun, J. J.; Dhaeze, K.; Mortier, W. J.; Vaughan, D. E. W. *J. Phys. Chem. Solids* **1989**, *5*, 469.
(15) Olson, D. *Zeolites* **1995**, *15*, 439.
(16) Feuerstein, M.; Hunger, M.; Engelhardt, G.; Amoureux, J. P. *Solid State NMR* **1996**, *5*, 95.
(17) Bein, T.; Schmiester, G.; Jacobs, P. A. *J. Phys. Chem.* **1986**, *90*, 4851.
(18) Huang, Y.-Y.; Anderson, J. R. *J. Catal.* **1975**, *40*, 143.
(19) Bein, T.; Schmidt, F.; Jacobs, P. A. *Zeolites* **1985**, *5*, 240.
(20) Mohana Rao, K.; Spotto, G.; Gugielminotti, E.; Zecchina, A. *Inorg. Chem.* **1989**, *28*, 243.
(21) Moller, K.; Borvornwattananont, A.; Bein, T. *J. Phys. Chem.* **1989**, *93*, 4562.
(22) de Vos, D. E.; Feijen, E. J. P.; Schoonheydt, R. A.; Jacobs, P. A. *J. Am. Chem. Soc.* **1994**, *116*, 4746.
(23) de Vos, D. E.; Thibault-Starzyk, F.; Jacobs, P. A. *Angew. Chem.* **1994**, *106*, 447.
(24) Li, G. Q.; Govind, R. *Inorg. Chem.* **1994**, *33*, 135.
(25) Paez-Mozo, E.; Gabriunas, N.; Maggi, R.; Acosta, D. D.; Ruiz, P.; Delmon, B. *J. Mol. Catal.* **1994**, *91*, 251.
(26) Páez-Mozo, E.; Gabriunas, N.; Lucaccioni, F.; Acosta, D. D.; Patrono, P.; La Ginestra, A.; Ruiz, P.; Delmon, B. *J. Phys. Chem.* **1993**, *97*, 12819.
(27) Schneider, R. L.; Howe, R. F.; Watters, K. L. *Inorg. Chem.* **1984**, *23*, 4600.
(28) Connaway, M. C.; Hanson, B. E. *Inorg. Chem.* **1986**, *25*, 1445.
(29) Andersson, S. L. T.; Howe, R. F. *J. Phys. Chem.* **1989**, *93*, 4913.
(30) Li, X.; Ozin, G. A.; Özkar, S. *J. Phys. Chem.* **1991**, *95*, 4463.
(31) Beagley, E.; Parrott, C. T.; Ulbrecht, V.; Young, G. C. *J. Mol. Struct.* **1979**, *52*, 47.
(32) Ozin, G. A.; Godber, J. *J. Phys. Chem.* **1989**, *93*, 878.
(33) Suib, S. L.; MacMahon, K. C.; Psaras, D. *Intrazeolite Chemistry*; Stucky, G. D., Dwyer, F. G., Eds.; ACS Symposium 218; American Chemical Society: Washington, DC, 1986; p 301.
(34) Dutta, P. K.; Thomson, M. A. *Chem. Phys. Lett.* **1986**, *131*, 435.
(35) Li, Z.; Mallouk, T. E. *J. Phys. Chem.* **1987**, *91*, 643.
(36) Lambert, J. B.; Finzel, R. B. *J. Am. Chem. Soc.* **1983**, *105*, 1954.
(37) Wilkinson, G. *Org. Synth.* **1956**, *36*, 31.
(38) Brauer, G. *Handbuch der Präparativen Anorganischen Chemie*, Ferd. Enke; Verlag: Stuttgart, 1962.
(39) Jolly, W. L. *Inorg. Synth.* **1968**, *11*, 120.
(40) Wemmer, D. E.; Ruben, D. J.; Pines, A. *J. Am. Chem. Soc.* **1981**, *103*, 28.
(41) Pines, A.; Gibby, M. G.; Waugh, J. S. *J. Chem. Phys.* **1973**, *59*, 569.
(42) Wemmer, D. E.; Pines, A. *J. Am. Chem. Soc.* **1981**, *103*, 34.
(43) Gibb, T. C. *J. Chem. Soc., Dalton Trans.* **1976**, 1237.
(44) Lyatifov, I. R.; Dhzafarov, S. M.; Babin, V. N.; Petrovskii, D. V.; Zagorevskii, V. D. *J. Organomet. Chem.* **1989**, *368*, 223.
(45) Lowery, M. D.; Wittebort, R. J.; Sorai, M.; Hendrickson, D. N. *J. Am. Chem. Soc.* **1990**, *112*, 4214.
(46) Singwi, K. S.; Sjölander, A. *Phys. Rev.* **1960**, *120*, 1092.
(47) Siebert, W.; Ruf, W.; Schaper, K.; Renk, T. *J. Organomet. Chem.* **1977**, *128*, 219.
(48) Bull, L. M.; Henson, N. J.; Cheetham, A. K.; Newsam, J. M.; Heyes, S. J. *J. Phys. Chem.* **1993**, *97*, 11776.
(49) Voss, V.; Boddenberg, B. *Surf. Sci.* **1993**, *298*, 241.
(50) Auerbach, S. M.; Henson, N. J.; Cheetham, A. K.; Metiu, H. I. *J. Phys. Chem.* **1995**, *99*, 10600.
(51) Auerbach, S. M.; Bull, L. M.; Henson, N. J.; Metiu, H. I.; Cheetham, A. K. *J. Phys. Chem.* **1996**, *100*, 5923.
(52) Vitale, G.; Mellot, C. F.; Bull, L. M.; Cheetham, A. K. *J. Phys. Chem. B* **1997**, *101*, 4559.
(53) Spiess, H. W. *NMR Basic Principles and Progress*; Diehl, P., Fluck, E., Kosfeld R., Eds.; Springer: Berlin, 1978.
(54) Germanus, A.; Kärger, J.; Pfeifer, H.; Samulevic, N. N.; Zdanov, S. P. *Zeolites* **1985**, *5*, 91.
(55) Aliev, A. E.; Harris, K. D. M.; Guillaume, F.; Barrie, P. J. *J. Chem. Soc., Dalton Trans.* **1994**, 3193.